Journal of Physics: Conference Series

Frequency-difference electrical impedance tomography: Phantom imaging experiments

To cite this article: Sujin Ahn *et al* 2010 *J. Phys.: Conf. Ser.* **224** 012152

Journal of Physics: Conference Series **224** (2010) 012152 doi:10.1088/1742-6596/224/1/012152

Frequency-difference electrical impedance tomography: phantom imaging experiments

Sujin Ahn[1], Sung Chan Jun[1,5], Jin Keun Seo[2], Jeehyun Lee[2], Eung Je Woo[3], and David Holder[4]
[1]Department of Information & Communications, Gwangju Institute of Science and Technology, Gwangju, Korea
[2]Department of Mathematics, Yonsei University, Seoul, Korea
[3]Department of Biomedical Engineering, Kyung Hee University, Yongin, Korea
[4]Department of Medical Physics, University College London, London, UK

E-mail: scjun@gist.ac.kr

Abstract. Frequency-difference electrical impedance tomography (fdEIT) using a weighted voltage difference has been proposed as a means to provide images of admittivity changes at different frequencies. This weighted difference method is an effective way to extract anomaly information while eliminating background effects by unknown boundary geometry, uncertainty in electrode positions and other systematic measurement artefacts. It also properly handles the interplay between conductivity and permittivity in measured boundary voltage data. Though the proposed fdEIT algorithm is promising for applications such as detection of hemorrhagic stroke and breast cancer, more validation studies are needed. In this paper, we performed two- and three-dimensional numerical simulations and phantom experiments. Backgrounds of imaging objects were either saline or carrot pieces suspended in saline. We used carrot pieces to simulate a more realistic frequency-dependent admittivity distribution. Test objects were banana, potato or conductive gel with known admittivity spectra. When the background was saline, both simple and weighted difference approaches produced reasonably accurate images. The weighted difference method yielded better images from two-dimensional imaging objects with background of carrot pieces. For the three-dimensional head-shaped phantom, the advantage of the weighted frequency difference method over the simple difference method is not as obvious as in the case of the two-dimensional phantom. It is unclear if this is due to measurement errors or limitations in the linear algorithm. Further refinement and validation of the frequency difference image reconstructions are currently in progress.

1. Introduction

Frequency-difference EIT (fdEIT) reconstructs images of admittivity differences between two frequencies using simultaneously acquired boundary current-voltage data. We use it when time-referenced data are not available, as in acute ischemic stroke in the brain or breast cancer. As a simple linear fdEIT method has been shown to be ineffective in adult human stroke, we have developed a weighted voltage difference method, in which changes in the background over frequency are corrected [1, 2]. The goal of this study was to evaluate its performance. Images produced with it, time difference

[5] To whom any correspondence should be addressed.

and simple frequency difference have been assessed with simulated data and that acquired in two- or three-dimensional tanks filled with saline or a background of complex conductivity.

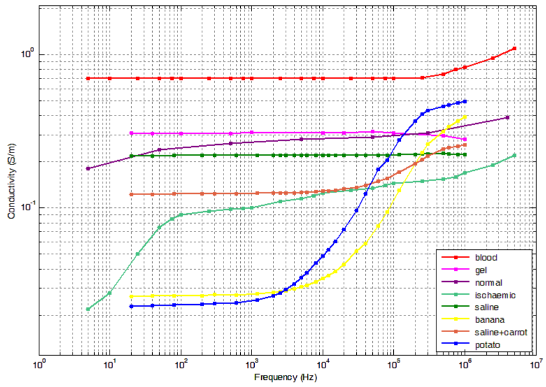

Figure 1. Conductivity spectra of blood [3], normal and ischemic brain tissues [3], and banana, potato, carrot, and gel.

(a) (b) (c)

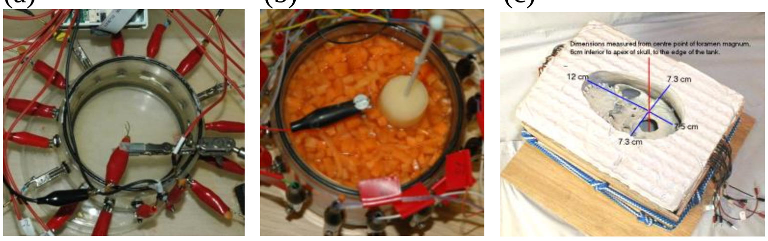

Figure 2.
(a) Two-dimensional cylindrical tank filled with saline, (b) the same tank filled with carrot pieces in saline and (c) three-dimensional head shaped tank.

2. Experimental design and methods

Images were reconstructed using time-difference (TD), simple frequency-difference (FD) and weighted frequency difference (WFD) methods from data produced either by simulation at 1, 5, 10, 50 and 100 kHz or from a two-dimensional cylindrical phantom and a three-dimensional head-shaped phantom filled with either saline or carrot pieces suspended in saline and with anomalies of a cylindrical piece of banana, potato or gel, with the diameter of each anomaly was 20% of the diameter of the tank. Biological materials are adopted since they have frequency-dependent conductivity spectra. The spectral properties of the mixture of saline and carrot pieces, potato and gel resembled those of normal, ischemic and haemorrhagic brain tissues, respectively (Figure 2). For the weighted frequency difference method, the reference frequency of $\omega_0/2\pi$ = 1 kHz was used to estimate an equivalent homogeneous admittivity. Tank data were acquired using a UCH Mk2.5 EIT system operating from 20 Hz to 1 MHz.

2.1 Direct impedance measurement

We measured conductivity spectra of saline, banana, potato and gel using an impedance analyzer (4284A, Agilent, USA) from 20 Hz to 1 MHz (Figure 2). Conductivity values of banana and carrot pieces in saline increased as frequency increased and those values of banana crossed that of saline at around 250 kHz. Conductivity of potato started increasing early and crossed that of saline at around 50 kHz.

2.2 Tank preparation

The diameter and height of the two-dimensional cylindrical tank were 10 and 8 cm, respectively. There were 16 electrodes equally spaced around its circumference. We filled it with either 0.1% saline or a mixture of carrot pieces (60%) and 0.1% saline (40%). We placed the banana anomaly as in figure 2(b) at the position of (2.5, 0) cm when the center of the phantom is denoted as (0, 0) cm. We placed the potato or gel anomaly at (-2.5, 0) cm. A head-shaped tank was made of silicon rubber and had 31 electrodes located at positions of the 10-20 EEG electrode placement system. It did not include a real human skull. The same anomaly settings including the banana anomaly in saline and the potato anomaly in the mixture of carrot pieces with saline were used.

3. Results

3.1. Numerical simulations

For images reconstructed from simulated data, acceptable images were produced for all modelled tanks by TD and WFD; with FD, images with the complex background were blurred for the two-dimensional case and inaccurate for the three-dimensional case.

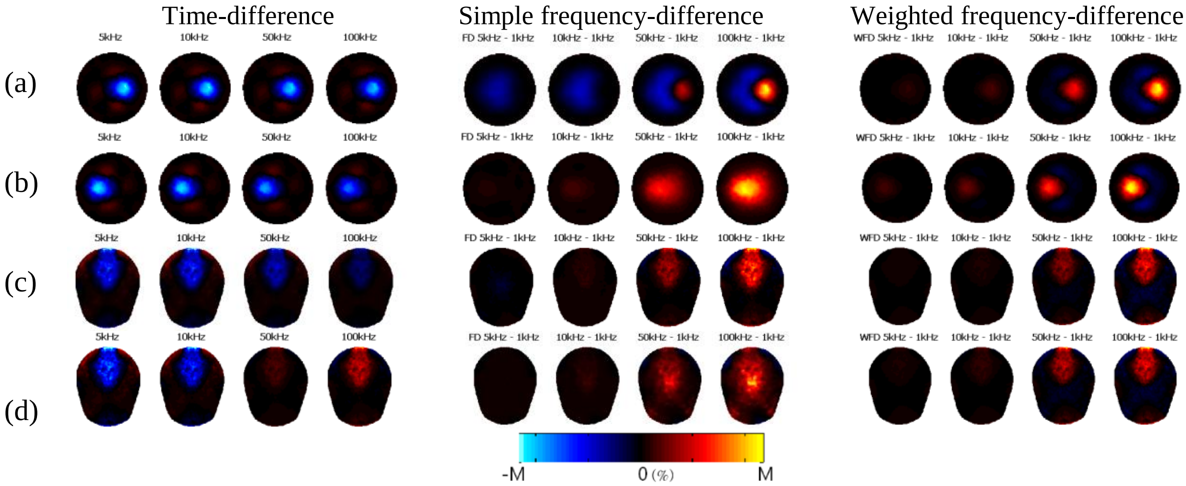

Figure 3. Reconstructed images from numerical simulation. The twelve images in each row are from the same anomaly setting. (a) The banana anomaly in the two-dimensional cylindrical phantom with the saline background. (b) The potato anomaly in the same two-dimensional phantom with the mixture of carrot pieces and saline as the background. (c) The banana anomaly in the saline background for the case of the three-dimensional head phantom. (d) The potato anomaly in the background of carrot pieces suspended in saline for the same head phantom. The pixel values represent percentile changes of conductivity.

3.2. Phantom experiments

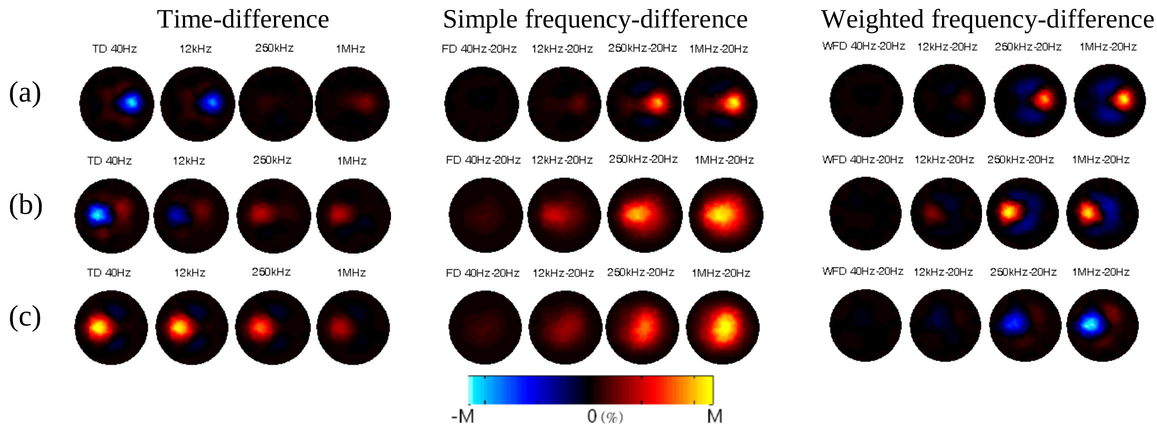

Figure 4. Reconstructed images of the two-dimensional cylindrical phantom. The twelve images in each row are from the same anomaly setting. (a) The banana anomaly in the saline background. (b) The potato anomaly in the background of carrot pieces suspended in saline. (c) The gel anomaly in the background of carrot pieces suspended in saline.

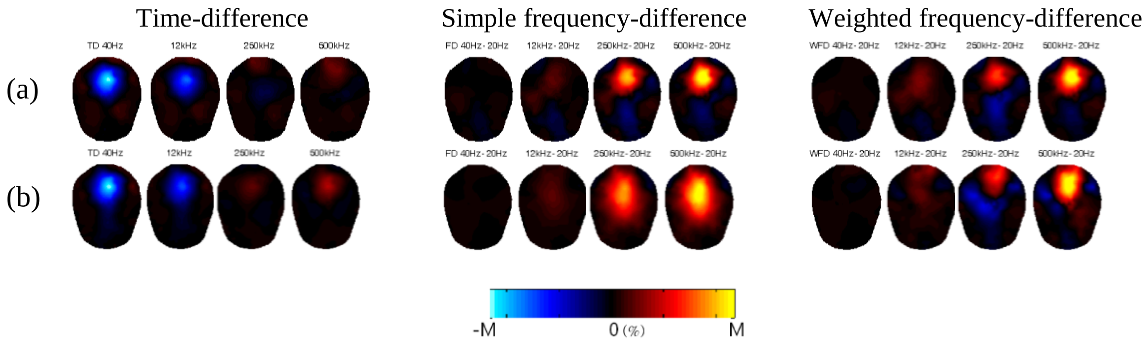

Figure 5. Reconstructed images of the three-dimensional head-shaped phantom. Twelve images in each row are from the same anomaly setting. (a) The banana anomaly in the saline background. (b) The potato anomaly in the background of carrot pieces suspended in saline.

For images collected in tanks, the findings are similar (Figure 4 and 5). With a saline background, the simple and weighted difference methods produced similar images. For the complex background, the weighted frequency-difference method performs better than the simple frequency-difference method. Blurred artifacts occurred around the perimeter of the anomaly since the conductivity values of the background as well as the anomaly changed nonlinearly with respect to frequency (Figure 4(b)). The weighted frequency-difference method minimized the artifacts and produced better localization of the anomaly. For the head-shaped phantom with one posterior anomaly, in the posterior the weighted frequency difference method again produced better images but the advantage is not as obvious as the two-dimensional case.

4. Conclusion

When the background conductivity does not change with frequency, the performance of the simple frequency difference method is comparable to that of the weighted frequency difference method. For the case of frequency-dependent background conductivity, the weighted frequency difference method produces better images in terms of its ability to localize an anomaly. However, its performance is degraded for the case of the three-dimensional head-shaped phantom. We plan to investigate effects of boundary geometry and electrode configuration. As shown in Jun et al [2], we could confirm that the weighted frequency-difference method is superior to the simple difference method in two-dimensional cases, but we need to further validate its applicability in three-dimensional case. As there were similar results with simulated and tank data, this is probably an intrinsic effect rather than due to limitations of the instrumentation.

Acknowledgement
This work was supported by NRF grant (2009-0071225) and the BioImaging Research Center at GIST. E J Woo was supported by the SRC/ERC program of MOST/KOSEF (R11-2002-103) and J K Seo and J Lee were supported by the WCU program (R31-2008-000-10049-0).

References
[1] J K Seo et al., Frequency-difference electrical impedance tomography (fdEIT): algorithm development and feasibility study, Physiol. Meas. 29 (2008) 929–944.
[2] S C Jun et al., Frequency-difference EIT (fdEIT) using weighted difference and equivalent homogeneous admittivity: validation by simulation and tank experiment. Physiol. Meas. 30 (2009) 1087–1099.
[3] C Gabriel et al., The dielectric properties of biological tissues: I, II, III., Phys.Med.Biol. 41 (1996) 2231-2293.
[4] L Fabrizi et al., An electrode addressing protocol for imaging brain function with electrical impedance tomography using a 16-channel semi-parallel system, Physiol. Meas. 30 (2009) S85-S101.